Struct Multidisc Optim (2005) 29: 304–311
DOI 10.1007/s00158-004-0485-x

INDUSTRIAL APPLICATIONS

J. Han · R. Itoh · S. Nishiyama · K. Yamazaki

Application of structure optimization technique to aluminum beverage bottle design

Received: 12 April 2004 / Revised manuscript received: 16 July 2004 / Published online: 26 October 2004
© Springer-Verlag 2005

Abstract This paper deals with shape optimization of two-piece aluminum beverage bottle bottoms by applying the structural optimization technique. Nonlinear finite element analyses were performed to study the influence of the design parameters on the buckling strength and the stiffness of the bottom under an axial load and internal pressure, respectively. On the basis of sensitivity analyses, the most effective dimensions are selected as design variables in the first stage design optimization, while the dimensions with relatively small influences are optimized in the secondary and following stages. In the design optimization of the bottom shape, the column strength is maximized subjected to the bottom growth and the axial displacement constraints, while the bulge strength is restricted to fall into a predetermined range. Optimizing the design variables progressively can avoid unrealistic geometrical connectivity problems during the arrangement of design points using the orthogonal array in the design-of-experiment, and can ensure the design space for the important design variables as well as the reduction of optimization cost.

Keywords Nonlinear structural response · Progressive optimization · Response surface approximation · Two-piece aluminum beverage bottle

1 Introduction

Aluminum beverage bottles (Fig. 1a) have been attracting more consumers because they have the advantages of regular aluminum beverage cans such as the high capability to be recycled as well as the advantages of PET bottles such as the capability to be resealed (Nishiyama 2001; Ueno 2003). Can makers are showing an increasing interest in two-piece (2-Pc) aluminum bottles because they can be manufactured by exiting equipment for regular 2-Pc cans. 2-Pc bottles and regular cans have a similar shape at the bottom but do not have the same structural performance requirements. High strength and stiffness are required, while the bulge strength of the bottle bottom is also expected to be lower than a limiting value so that the bottom may buckle before the cap flies off due to an unexpected high internal pressure. In order to improve the structural performance of regular 2-Pc can bottoms, studies on the influence of the geometrical shape have been done experimentally and numerically in recent years (Trageser and Dick 1988, 1991; Han et al. 2004). Reference Trageser and Dick (1991) has utilized two-level full factorial design in experimental design to predict the influence of geometrical parameters. Structural optimization technology has been applied to the optimization of crushing characteristics of triangulated aluminum beverage cans (Han et al. 2004), but no application has been found for 2-Pc bottles.

On the other hand, it is becoming popular for engineers to apply the response surface approximation (RSA) method to carry out optimization based on finite element analysis because RSA is included in structure optimization software packages. Research on how to improve RSA and how to ap-

J. Han · R. Itoh · S. Nishiyama
Technical Development Department, Aluminum Company, Mitsubishi Materials Corporation, 1500 Suganuma, Oyama-Cho, Sunto-Gun, Shizuoka 410-1392, Japan
E-mail: hanjing@mmc.co.jp

K. Yamazaki (✉)
Department of Human and Mechanical Systems Engineering, Kanazawa University, 2-40-20 Kodatsuno, Kanazawa, Ishikawa 920-8667, Japan
E-mail: yamazaki@t.kanazawa-u.ac.jp

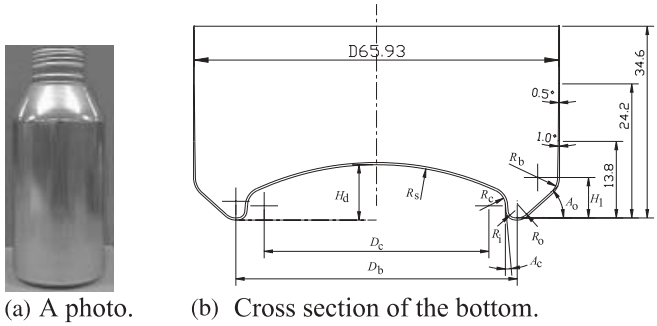

(a) A photo. (b) Cross section of the bottom.

Fig. 1 A two-piece aluminum beverage bottle

ply RSA effectively have been done continually using techniques such as neural networks, genetic algorithms (GA), fuzzy theory, optimization methodology and so on (Kroo et al. 1994; Burgee et al. 1996; Rodriguez et al. 1998; Fellini et al. 2001; Han and Yamazaki 2000, 2003; Yamazaki and Han 1998). However, no structural optimization technique has been applied to design beverage bottles directly including the continually nonlinear structural response. When applying RSA to complex geometry, people usually tend to define many dimensional factors as design variables and to optimize them simultaneously. In many cases, the factors have very different levels of influence on responses and are sometimes independent of each other. Simultaneous optimization of many factors always causes a reduction in the changeable ranges of design variables due to interaction between parameters. This paper addresses the solution of optimization problems with many geometrical factors affecting the nonlinear responses of the system. The design variables are optimized progressively depending on their effectiveness levels. At first the effectiveness level of factors are evaluated qualitatively on the basis of numerical estimations or experimental data. The factors that govern the nonlinear responses of the system are optimized first, while the factors that do not have much influence over the response and that are independent of other factors are postponed to be included in the design variables. On the basis of the shape designed optimally in the previous stage, the optimization for the remaining design variables is then performed in the secondary and following stages. By applying this proposed method, the shape of a 2-Pc aluminum bottle bottom is optimized to achieve the maximum column strength so that the weight of the bottle may be reduced in the further bottle design.

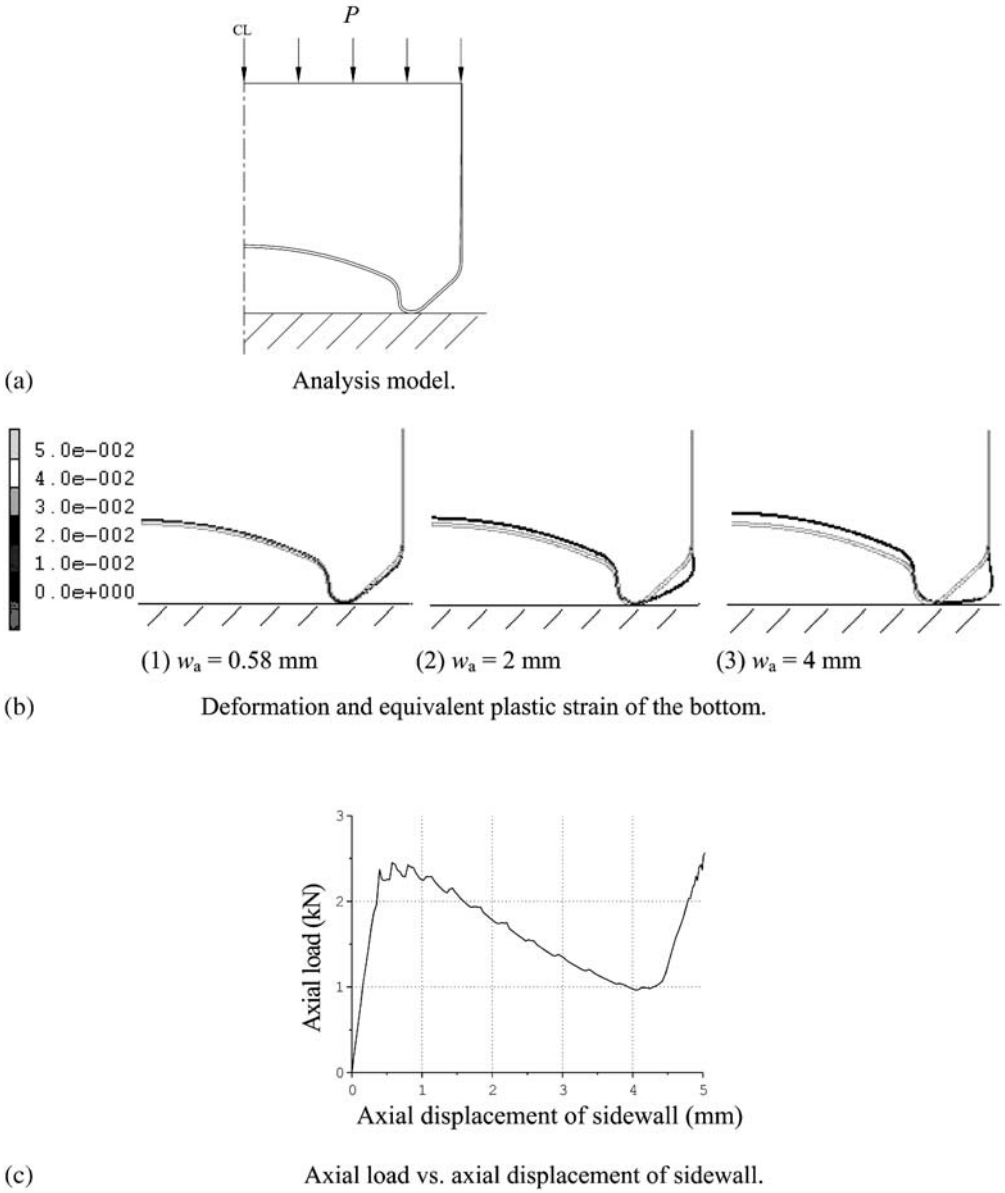

Fig. 2 Numerical analysis under an axial load

2 Numerical estimation of the structural performance of bottle bottoms

The cross section of the bottle bottom model is shown in Fig. 1b. The baseline parameters for the bottom shape are given as: outer nose radius $R_o = 2.50$ mm, counter sink angle $A_c = 5.22°$, dome depth $H_d = 10.00$ mm, inner transition radius $R_c = 3.00$ mm, spherical radius $R_s = 52.00$ mm, lower body radius $R_b = 3.60$ mm, transition center diameter $D_c = 40.65$ mm, bottom height $H_1 = 7.30$ mm, taper angle $A_o = 42.00°$, inner nose radius $R_i = 1.68$ mm and base diameter $D_b = 50.95$ mm. The thickness of the bottom and top parts of the sidewall are given as $T = 0.400$ mm and $T_1 = 0.135$ mm, respectively. The material model used is an elasto-plastic von Mises material with isotropic hardening. Young's modulus $E = 70$ GPa, Poisson's ratio $\nu = 0.33$ and yielding stress $\sigma_0 = 260$ MPa are assumed for bottle products. The cross section of the bottom is descritized into four-node axisymmetric elements, and a nonlinear finite element code, MSC.MARC, is utilized to analyze the structural performance of bottle bottoms under an axial load and an internal pressure, respectively.

2.1 Finite element analysis of bottom under axial load

Figure 2a shows an analysis model. An axial load is applied to the top of sidewall and a rigid wall supports a part of the bottle bottom. A deformation process and equivalent plastic

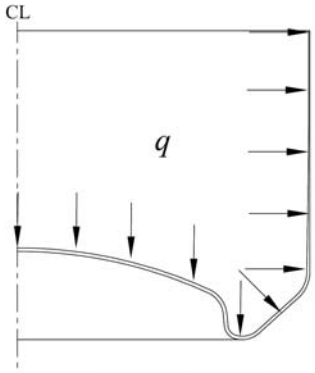

(a) Analysis model.

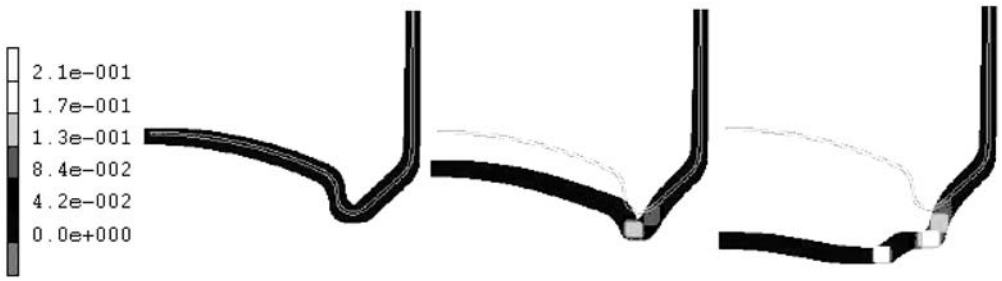

(1) $w_b = 0.16$ mm (2) $w_b = 2.6$ mm (3) $w_b = 6.0$mm

(b) Deformation and equivalent plastic strain of the bottom.

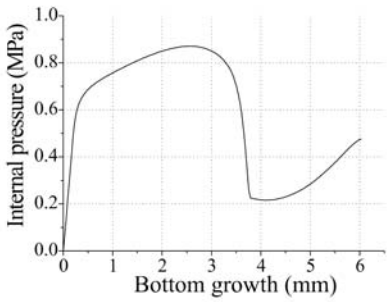

(c) Internal pressure vs. bottom growth.

Fig. 3 Numerical analysis under internal pressure

Table 1 Dimensions of the analysis models

Model	R_o mm	A_c deg	H_d mm	R_c mm	R_s mm	R_b mm	D_c mm	H_1 mm	A_o deg	R_i mm	D_b mm
0	2.5	5.22	10	3.0	52	3.6	40.65	7.30	42	1.68	50.95
1	0.8	–	–	–	–	–	–	–	–	2.40	52.26
2	1.6	–	–	–	–	–	–	–	–	2.06	51.64
3	3.2	–	–	–	–	–	–	–	–	1.39	50.40
4	–	2.00	–	–	–	–	–	–	–	1.73	–
5	–	8.00	–	–	–	–	–	–	–	1.62	–
6	–	–	–	–	–	3.0	–	7.03	–	–	–
7	–	–	–	–	–	4.2	–	7.57	–	–	–
8	1.2	–	–	–	–	–	–	–	–	2.23	51.94
9	1.0	–	–	–	–	–	–	–	–	2.31	52.10
10	1.0	–	9	1.0	–	–	44.62	–	–	2.31	–
11	1.0	–	9	0.5	–	–	45.56	–	–	2.31	–
12	1.0	–	9	0.5	50	–	45.60	–	–	2.31	–
13	1.0	–	9	0.5	54	–	45.52	–	–	2.31	–
14	1.0	–	–	–	–	–	–	7.75	45	–	–

strain distribution of the bottom are simulated in Fig. 2b. It is found that the lower body arc of the bottom deforms outward while the sidewall sinks down. The outer nose arc gradually becomes flat and comes into contact with the rigid wall. The dome rises up without obvious deformation. The plastic strain region starts from the inner nose arc part and spreads out to both sides, and the plastic strain region in the lower body arc expands downward. Figure 2c gives a curve of axial load versus the axial displacement of the sidewall. The column strength of the bottom $P_{cr} = 2.5$ kN is estimated for the baseline model. The axial downward displacement at the top of sidewall $w_a = 0.15$ mm when the axial force $P = 1.0$ kN and $w_{acr} = 0.57$ mm when column buckling occurred at the bottom.

2.2 Finite element analysis of bottom under internal pressure

As shown in Fig. 3a, an internal pressure is applied to the bottom. The axial movements of nodes at the top of the sidewall are restricted. A deformation process and equivalent plastic strain distribution of the bottom are simulated in Fig. 3b. The plastic strain region starts from the inner nose arc part and expands to both sides. Figure 3c shows a curve of the internal pressure versus the bottom growth, which is defined as the axial extension. The bulge strength of the bottom $q_{cr} = 0.87$ MPa is estimated for the baseline model. The bottom growth $w_b = 0.16$ mm when the internal pressure is 0.4 MPa, and $w_{bcr} = 2.6$ mm when buckling occurred at the bottom.

2.3 Influence of geometrical parameters

In order to grasp the influence of geometrical dimensions on the structural behavior, several models with different combinations of dimensions have been studied. The main dimensions of each model are listed in Table 1, where empty columns mean that values are the same as those of the baseline design, Model 0. When some dimensions are changed,

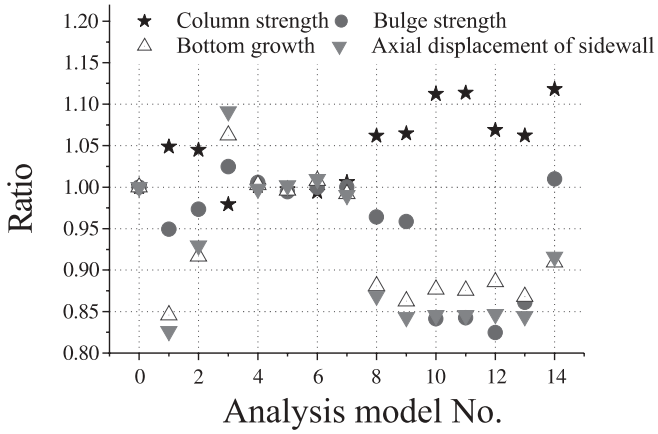

Fig. 4 Analysis results

related dimensions must be adjusted accordingly in order to keep geometrical connectivity of the bottle bottom. The ratios of the strength and stiffness of each model to those of the baseline model are compared in Fig. 4. From this comparison of results, the influence of the dimensions on the structural performance can be partially understood.

3 Optimization of bottom shape

3.1 Progressive optimization method based on RSA

This paper proposes a progressive optimization concept to optimize design problems with many design variables in complex geometrical relations. All design variables are optimized progressively rather than simultaneously, and the order of priority of design variables is dependent on their geometrical characteristics, sensitivity to the response, and independency. The following optimization steps are suggested in this paper:

i) Select the design variables for each stage of the optimization. In the case that the relations among the design variables are complex and if the design variables are optimized simultaneously, the initial design space must be restricted to a small range in order to avoid unreasonable geometrical shapes caused by a combination of design variables. It is difficult to pre-set the design space properly and it is undesirable to limit the upper and lower bounds of the important design variables for such a reason. In addition, their influence can be understood more easily if design variables of relatively little effectiveness and independency are optimized in the secondary and following stages. Therefore, it is better to determine the design variables for each stage based on numerical estimations, experimental results and various restrictions on practical production.
ii) Arrange the design points and perform the finite element analysis. After the design space is defined, an orthogonal array in the design-of-experiment is used to arrange the design points and the finite element code is utilized to implement the structural analysis.
iii) Calculate the relative influence ratio of design variables. In contrast to the traditional RSA based on orthogonal experimental design, the relative influence ratio, instead of the variance ratio, is calculated. Consider a problem with two design variables A and B of a and b design levels in equal intervals, the sum of squares to the response y are calculated using (1), (2).

$$S_{\mathrm{A}} = \sum_{i=1}^{a} \frac{y_{i\cdot}^2}{b} - \left(\sum_{i=1}^{a} \sum_{j=1}^{b} y_{ij} \right)^2 /ab \tag{1}$$

$$S_{\mathrm{B}} = \sum_{j=1}^{b} \frac{y_{\cdot j}^2}{a} - \left(\sum_{i=1}^{a} \sum_{j=1}^{b} y_{ij} \right)^2 /ab \tag{2}$$

The relative influence ratios are then calculated using (3), (4)

$$r_{\mathrm{A}} = S_{\mathrm{A}} / \max\{S_{\mathrm{A}}, S_{\mathrm{B}}\} \tag{3}$$

$$r_{\mathrm{B}} = S_{\mathrm{B}} / \max\{S_{\mathrm{A}}, S_{\mathrm{B}}\} \tag{4}$$

A design variable with a smaller influence ratio is not disregarded but is used to make a fine adjustment to the optimization solution in the later optimization processes.
iv) Construct the response surfaces and perform the optimization. The response surface approximation technique is then applied to generate an approximate response surface in terms of the selected design variables. The numerical optimization program is then used to perform the optimization calculation based on the response surfaces. If it is necessary to move the design space, according to judgment based on the optimization results, then repeat the calculations from Step ii).
v) Move to the secondary stage of optimization. On the basis of the optimization results obtained in the previous stage, optimization calculations are repeated from Step i). If all effective geometrical factors are optimized or further optimization is not necessary when considering the cost, finish the whole optimization processes.

3.2 Formulation of the optimization problem

The objective of the optimization is to maximize the column strength of the bottom. The bulge strength is restricted within prescribed limits, and the bottom growth w_b when the internal pressure is 0.4 MPa as well as the axial displacement of the sidewall w_a when the axial load is 1 kN are constrained to be lower than the allowable maximum values $w_{b\max}$ and $w_{a\max}$, respectively. The geometrical dimensions of the bottom are selected as the design variables. The problem is then posed as:

$$\text{Find design variables:} \quad X = \{x_i\}, \quad i = 1, \ldots, n \tag{5}$$

(n: the number of design variables)

$$\text{maximize} \quad f = P_{cr}(X), \tag{6}$$

subject to

$$g_1 = Q_{\min}/Q(X) - 1 \le 0, \tag{7}$$

$$g_2 = Q(X)/Q_{\max} - 1 \le 0, \tag{8}$$

$$g_3 = w_b(X)/w_{b\max} - 1 \le 0, \tag{9}$$

$$g_4 = w_a(X)/w_{a\max} - 1 \le 0, \tag{10}$$

$$x_i^L \le x_i \le x_i^U, \quad i = 1, \ldots, n \tag{11}$$

where $Q_{\max}$, $\mathrm{Q}_{\min}$ are the allowable upper and lower bounds of the bulge strength, and x_i^U and x_i^L are the upper and lower bounds of design variable i, respectively.

3.3 Numerical example

The bottom considered in this paper is optimized to achieve maximum column strength. The bulge strength is kept within a range of 0.70 MPa to 0.75 MPa, and $w_{a\max} = w_{b\max} = 0.1$ mm. In the first stage, dimensions D_b, R_o, H_d, R_s, R_i, and A_c are selected as the design variables with upper bounds of 56 mm, 3 mm, 10.5 mm, 54 mm, 2.1 mm, 8° and lower bounds of 52 mm, 1 mm, 9.5 mm, 50 mm, 1.5 mm and 4° based on the relative influence ratios. R_b and H_1 are kept the same as the baseline design, and A_o is dependent on D_b and R_o. In order to keep geometrical connectivity, a circle C is defined that forms an inner tangent to circle S and is tangent to lines AE and FE, as shown in Fig. 5, where line AE is a tangent line of circle F, and point E is a tangent point. Hence, R_c and D_c depend on the design variables D_b, H_d, R_s, R_i, and A_c. The structural analyses are performed for 27 design points that are arranged using the orthogonal array L_{27} as provided in Table 2. The ratios of the numerical results of each design point to that of the baseline are compared in Fig. 6a. The relative influence ratios of each design variable are shown in Fig. 6b. It can be

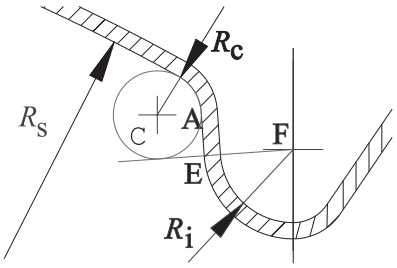

Fig. 5 Definition of inner transition

Table 2 Design points in the first stage

Design point	D_b	R_o	H_d	R_s	R_i	A_c
1	52	1	9.5	50	1.5	4
2	52	1	9.5	50	1.8	6
3	52	1	9.5	50	2.1	8
4	52	2	10.0	52	1.5	4
5	52	2	10.0	52	1.8	6
6	52	2	10.0	52	2.1	8
7	52	3	10.5	54	1.5	4
8	52	3	10.5	54	1.8	6
9	52	3	10.5	54	2.1	8
10	54	1	10.0	54	1.5	6
11	54	1	10.0	54	1.8	8
12	54	1	10.0	54	2.1	4
13	54	2	10.5	50	1.5	6
14	54	2	10.5	50	1.8	8
15	54	2	10.5	50	2.1	4
16	54	3	9.5	52	1.5	6
17	54	3	9.5	52	1.8	8
18	54	3	9.5	52	2.1	4
19	56	1	10.5	52	1.5	8
20	56	1	10.5	52	1.8	4
21	56	1	10.5	52	2.1	6
22	56	2	9.5	54	1.5	8
23	56	2	9.5	54	1.8	4
24	56	2	9.5	54	2.1	6
25	56	3	10.0	50	1.5	8
26	56	3	10.0	50	1.8	4
27	56	3	10.0	50	2.1	6

concluded that design variable 1 (D_b) influences the strength of the bottom whereas design variable 2 (R_o) significantly affects the stiffness. Second-order polynomial functions of the column strength, bulge strength, axial displacement of sidewall as well as bottom growth are approximated based on the numerical estimations. The approximated optimization problem is then solved by mathematical programming. The optimum values for the design variables are obtained as $D_b, = 56.00$, $R_o = 1.00$ mm, $H_d = 10.27$ mm, $R_s = 51.49$ mm, $R_i = 1.50$ mm, and $A_c = 5.94°$. Then, the objective value reaches 3.8 kN, and the constraints are $g_1 = -4.2 \times 10^{-2}$, $g_2 = -2.54 \times 10^{-2}$, $g_3 = 2.91 \times 10^{-3}$ and $g_4 = -2.71 \times 10^{-1}$. From the optimization result in the first stage, it is found that the design variables D_b and R_o adhered to the upper or lower bounds, and the remaining design variables of smaller influence adjust the optimum point. The numerical simulation was performed for the optimized model to confirm that the error was smaller than 5%,

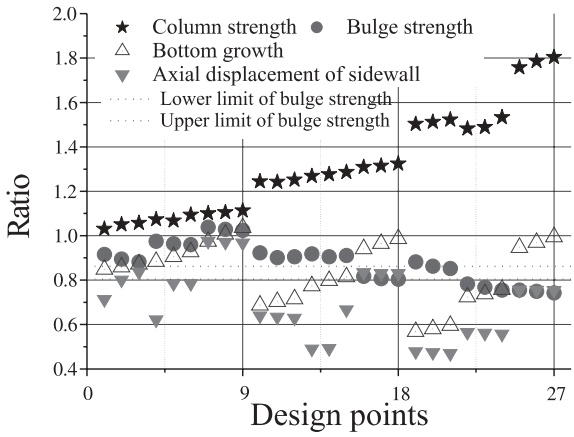

(a) Numerical results at each design point.

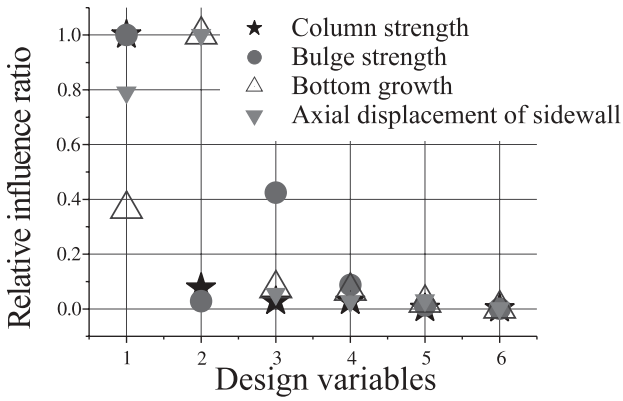

(b) Relative influence ratio of each design variable

Fig. 6 Analysis results in the first stage

Table 3 Design points in the second stage

Design point	A_o (deg)	R_b (mm)
1	54.2	3.2
2	54.2	3.6
3	54.2	4.0
4	55.6	3.2
5	55.6	3.6
6	55.6	4.0
7	57.0	3.2
8	57.0	3.6
9	57.0	4.0

and the column strength $P_{cr} = 3.7$ kN, the bulge strength $q_{cr} = 0.76$ MPa, $w_b = 0.095$ mm and $w_a = 0.074$ mm were estimated.

In the second stage, A_o and R_b are selected as the design variables, with upper bounds of 57.0° and 4.0 mm and lower bounds of 54.2° and 3.2 mm. H_1 is constrained to be lower than 7.7 mm in order to keep a large print area on the sidewall, i.e. the fifth constraint $g_5 = H_1/7.7 - 1 \leq 0$ is added. Referring to Fig. 1b, H_1 can be defined by the design variables using (12).

$$H_1 = R_b\sqrt{m_3^2+1}+m_3x_b+k_1 \tag{12}$$

where, $x_b = [R_b(\sqrt{m_3^2+1}-\sqrt{m_4^2+1})+k_1-k_2]/(m_4-m_3)$, $m_3=\tan A_o$, $m_4=\tan 89°$, $k_1=-R_o\sqrt{m_3^2+1}+y_o-m_3x_o$, $k_2=y_G-m_4x_G$, $x_G=65.93/2-D_b/2-(24.2-13.8)\tan 0.5° = 32.874-D_b/2$, $y_G=13.8$, $x_o=0$ and $y_o=R_o$.

The orthogonal array L_9 is used to arrange design points in the second optimization stage as provided in Table 3, and ratios of numerical estimations to the optimum solution obtained in the first stage are shown in Fig. 7. It is found that, by increasing the design variable A_o, the bulge strength becomes a little larger than the limiting value, but the column strength and the stiffness may increase significantly. So the limiting value of bulge strength is changed

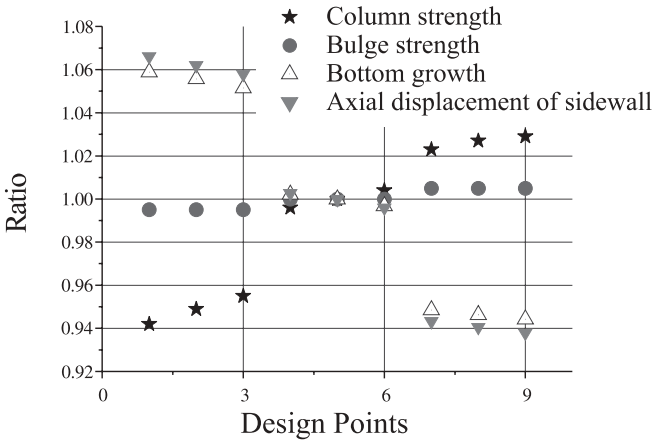

Fig. 7 Analysis results in the first stage

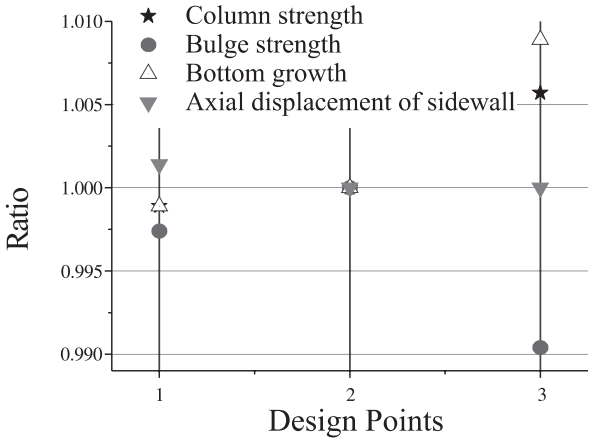

Fig. 8 Numerical results in the third stage

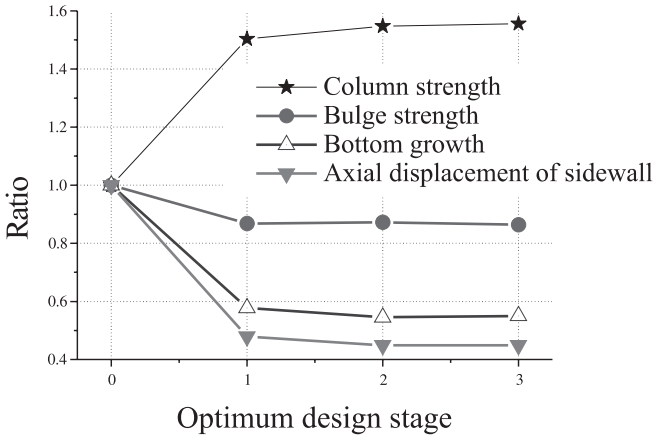

Fig. 9 The process of optimum design

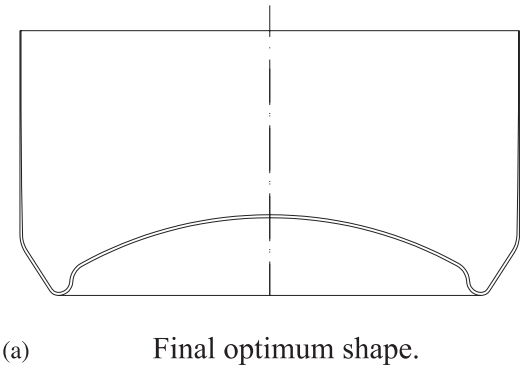

(a) Final optimum shape.

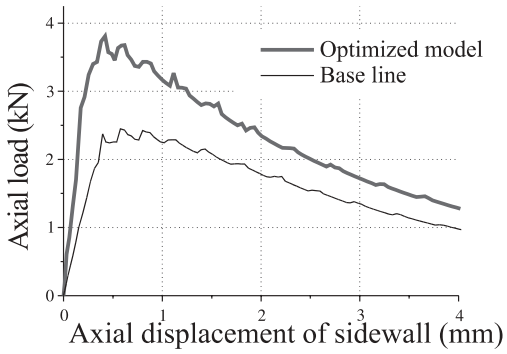

(b) Axial load vs. displacement.

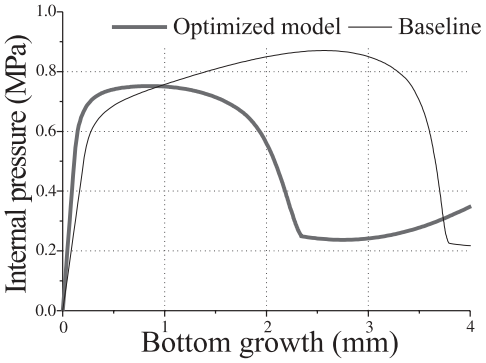

(c) Internal pressure vs. bottom growth.

Fig. 10 Comparison between optimized model and baseline design

to 0.76 MPa and the optimization results yield an objective value of 3.8 kN with constraints of $g_1 = -7.8 \times 10^{-2}$, $g_2 = -1.3 \times 10^{-3}$, $g_3 = -1.0 \times 10^{-1}$, $g_4 = -3.0 \times 10^{-1}$, $g_5 = -1.5 \times 10^{-3}$ when $A_o = 57°$ and $R_b = 4.0$ mm. Although two design variables attached to the bounds, the design space cannot be moved because the H_1 constraint function worked and the optimization process is finished.

In the third stage, on the basis of the optimum model obtained in the previous optimization stages where $R_c = 1.03$ mm, two additional design points with $R_c = 0.8$ and 2.5 mm are studied and compared with the optimum model obtained in the second stage, as shown in Fig. 8. Design analysis arranged by an orthogonal array is not necessary because R_c has a monotonous influence on the column strength. The third design point is accepted as the final optimum model.

The optimized bottles in the three optimization stages show a 50%, 4% and 1% increase in column strength subject to the constraints, respectively (Fig. 9). Since the optimization results are not improved much in the second and third stages, these two stages may be ignored in practical designs so that the optimization cost may be reduced. The optimum shape is illustrated in Fig. 10a, with final optimum dimensions of $R_o = 1.00$ mm, $A_c = 5.94°$, $H_d = 10.27$ mm, $R_c = 2.50$ mm, $R_s = 51.49$ mm, $R_b = 4.00$ mm, $D_c = 47.20$ mm, $H_1 = 7.69$ mm, $A_o = 57.00°$, $R_i = 1.50$ mm and $D_b = 56.00$ mm. Curves of the axial load versus axial displacement of the sidewall and internal pressure versus bottom growth are shown in Fig. 10b,c. The column strength $P_{cr} = 3.8$ kN, the bulge strength $q_{cr} = 0.75$ MPa, $w_b = 0.091$ mm and $w_a = 0.070$ mm were estimated numerically for the final optimum bottom.

4 Conclusions

A progressive design variable optimization method based on RSA was proposed and applied to optimize the shape of aluminum beverage bottle bottoms. A result with a 55% increase in column strength was obtained. The progressive optimization method can help designers to understand the optimization problem more clearly, make the optimization problem easier, and can obtain better solutions during progressive optimum design. The computational cost can also be minimized. The method proposed can be applied to not only beverage bottle designs but also to other complex industrial design problems including nonlinear structural responses such as optimum design of a vehicle against crash.

References

Burgee S, Giunta AA, Narducci R, Watson LT, Grossman B, Haftka RT (1996) A coarse grained parallel variable-complexity multidisciplinary optimization paradigm. Int J Supercomput Appl High Perform Comput 10(4):269–299

Fellini R, Kim HM, Kokkolaras M, Michelena N, Papalambros PY (2001) Target cascading for design of product families. Proceedings of the 4th Congress on Structural and Multidisciplinary Optimization, Dalian, China

Han J, Yamazaki K, Nishiyama S (2004) Optimization of the crushing characteristics of triangulated aluminum beverage cans. Struct Multidisc Optim 28(1):47–54

Han J, Yamazaki K (2003) Crashworthiness optimization of S-shape square tubes. Int J Vehicle Des 31(1):72–85

Han J, Yamazaki K (2000) A study on maximization of dynamic crushing energy absorption of square tubes with and without stiffener. JSME Int J Ser A 43(2):138–145

Kroo I, Altus S, Braun B, Gage P, Sobieski I (1994) Multidisciplinary optimization methods for aircraft preliminary design. Proceedings of the 5th AIAA /USAF/NASA/ISSMO Symposium on Multidisciplinary Analysis and Optimization, AIAA, pp94–4325

Nishiyama S (2001) Development and future subjects of aluminum beverage cans. Packpia 2:10–15 (in Japanese)

Rodriguez JF, Renaud JE, Watson LT (1998) Trust region augmented Lagrangian methods for sequential response surface approximation and optimization. J Mech Des 120:58–66

Trageser AB, Dick RE (1988) Aluminum can design using finite element methods. Proceedings of the SME Can Manufacturing Technical Symposium, Chicago

Trageser AB, Dick RE (1991) Beverage can structural analysis and automation. Proceeding of Design Productivity International Conference

Ueno H (2003) Drinks cans with customer convenience. The Canmaker Summit, Singapore

Yamazaki K, Han J (1998) Maximization of the crushing energy absorption of tubes. Struct Optim 16(1):37–46